

Hidden nonlinear optical susceptibilities in linear polaritonic spectra

Arghadip Koner¹ and Joel Yuen-Zhou^{1,*}

¹*Department of Chemistry and Biochemistry, University of California San Diego, La Jolla, California 92093*

(Dated: November 19, 2024)

Linear spectra of molecular polaritons formed by N molecules coupled to a microcavity photon mode are usually well described by classical linear optics, raising the question of where the expected nonlinear effects in these strongly coupled systems are. In this work, we derive a general expression for the polaritonic linear spectra that reveal previously overlooked finite-size quantum corrections due to vacuum-mediated molecular Raman processes. Using a $1/N$ expansion, we demonstrate that these nonlinearities are suppressed in typical low-Q cavities due to an emergent timescale separation in polariton dynamics yet manifest in high-Q single-mode cavities where the photon loss is comparable to the single-molecule light-matter coupling strength.

Polaritons have garnered significant attention in the last decade due to their promise to manipulate matter degrees of freedom (DOF) via coupling to a confined electromagnetic mode. They have offered a plethora of promising applications like enhanced energy transport [1–3], modification of chemical reactions [4, 5], and room temperature lasing [6, 7]. For molecular systems, strong coupling (SC) is typically realized through the interaction of an ensemble of $N \approx 10^6 - 10^{12}$ molecules with a microcavity mode [8]. The multiple exchanges of excitation between the electromagnetic mode and the matter optical polarization (see Fig 1a) are expected to induce nonlinear optical transitions in the molecules. However, recent studies suggest that several polaritonic phenomena can be replicated using appropriately shaped lasers, causing polaritons to sometimes act just as optical filters [9]. This effect is evident in the linear response of polaritons, which is well described using classical linear optics methods, such as transfer matrices, with the molecular optical constants as the only material input [10–16]. This classical linear optics description raises a fundamental question: what happened to the nonlinearities anticipated in the SC regime? The answer to this question is also key to uncovering genuine cavity-induced effects beyond classical optics.

In this letter, we solve this apparent contradiction by obtaining a general expression for the linear response of molecular polaritons, which evidences that the classical optical description is only correct in the thermodynamic limit ($N \rightarrow \infty$) and, in fact, there is a previously overlooked hierarchy of (finite-size) $1/N$ corrections containing signatures of nonlinear molecular processes like Raman scattering mediated by quantum vacuum fluctuations of the cavity. These corrections are small due to an emergent separation of timescales in polariton dynamics and are usually excluded from the spectra due to limited resolution in the low-Q cavities typically used in experiments. They manifest in high-Q single-mode cavities where the cavity decay rate κ becomes comparable to the single molecule coupling λ .

Model.—We consider a photonic cavity with a single-

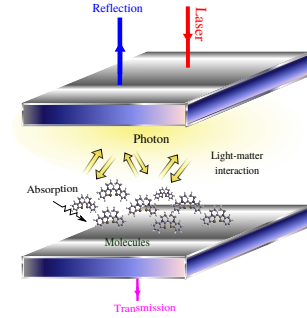


FIG. 1. Strong coupling between a cavity photon and molecular optical polarization leads to multiple exchanges of excitation between light and matter. We explore the conditions under which these exchanges lead to nonlinear optical processes in the molecules, even at linear order in the incoming photon field.

mode of frequency ω_{ph} coupled to N non-interacting molecules. Starting from a permutationally invariant initial state at zero temperature, the setup is described by a bosonic Hamiltonian at all times [Supplemental material: Sec. S1] [17–22],

$$H = \left[\hbar\omega_{\text{ph}}a^\dagger a + \hbar \sum_j \omega_{g,j} b_j^\dagger b_j + \hbar \sum_j \omega_{e,j} B_j^\dagger B_j \right] + \left[-\hbar\lambda \sum_{jj'} \langle \varphi_{j'}^{(e)} | \varphi_j^{(g)} \rangle a b_j B_{j'}^\dagger - \text{h.c.} \right], \quad (1)$$

with operators a that annihilates a cavity excitation (photon), and $b_j(B_{j'})$ that annihilate a molecule in vibronic state $|g, \varphi_j^{(g)}\rangle (|e, \varphi_{j'}^{(e)}\rangle)$; $j(j')$ label the vibrational level in the ground (excited) electronic state. To compute linear response, we project the Hamiltonian to the first excitation manifold, where it admits a block tridiagonal

representation [23]:

$$H_1 = \begin{pmatrix} \mathbf{H}_{\text{ph},0} & \mathbf{V}_0 & 0 & \dots & 0 & 0 & 0 \\ \mathbf{V}_0^\dagger & \mathbf{H}_{e,0} & \mathbf{v}_0 & \dots & 0 & 0 & 0 \\ 0 & \mathbf{v}_0^\dagger & \mathbf{H}_{\text{ph},1} & \mathbf{V}_1 & 0 & 0 & 0 \\ \vdots & \vdots & \vdots & \ddots & \vdots & \vdots & \vdots \\ 0 & 0 & 0 & \dots & \mathbf{V}_{N-1}^\dagger & \mathbf{H}_{e,N-1} & \mathbf{v}_{N-1} \\ \vdots & \vdots & \vdots & \vdots & 0 & \mathbf{v}_{N-1}^\dagger & \mathbf{H}_{\text{ph},N} \end{pmatrix}. \quad (2)$$

Here $\mathbf{H}_{\text{ph},n}$ denotes the effective cavity single-photon Hamiltonian for the subspace where n molecules have phonons in the ground state (e.g. $\mathbf{H}_{\text{ph},0} = (\omega_{\text{ph}} - i\kappa/2)|1_{\text{ph},0}\rangle\langle 1_{\text{ph},0}|$ for a cavity excitation with all molecules in $|g, \varphi_0^{(g)}\rangle$), and $\mathbf{H}_{e,n}$ corresponds to the photonless subspace with one molecule excited and n other molecules having phonons in the ground state [24, 25]. The off-diagonal elements reveal the crucial timescale separation: couplings \mathbf{V}_n drive the collective $\mathcal{O}(\lambda\sqrt{N})$ ‘Rayleigh’ transitions that conserve the number of molecules with ground state phonons, and \mathbf{v}_n mediate the single-molecule $\mathcal{O}(\lambda)$ ‘Raman’ transitions that create/destroy the phonons in one of the molecules [26].

The linear spectroscopic observables of cavity-coupled systems (absorption, reflection, transmission) can be entirely expressed in terms of the photon Green’s function $D_N^R(\omega) = \langle 1_{\text{ph},0} | \mathbf{G}(\omega) | 1_{\text{ph},0} \rangle$ [Supplemental material: Sec. S2], where $\mathbf{G}(\omega) = \frac{1}{\omega - \mathbf{H}_1 + i0^+}$. In particular,

the absorption is given by [16],

$$A(\omega) = -(\kappa/2)[\kappa|D_N^R(\omega)|^2 + 2\text{Im} D_N^R(\omega)], \quad (3)$$

To compute $D_N^R(\omega)$, we exploit the block tridiagonal structure of H_1 and use standard techniques for matrix Green’s functions of systems with nearest neighbor couplings [see Supplemental material: Sec. S3] [27–29].

Rewriting the Hamiltonian $H_1 = \begin{pmatrix} \mathbf{H}_{\text{ph},0} & \mathbf{V}_0 \\ \mathbf{V}_0^\dagger & \tilde{\mathbf{H}}_{e,0} \end{pmatrix}$ yields

$$D_N^R(\omega) = \frac{1}{\omega - \omega_{\text{ph}} + i\kappa/2 - \Sigma_{e,0}(\omega)}, \quad (4)$$

where $\Sigma_{e,0}(\omega) = \mathbf{V}_0(\omega - \tilde{\mathbf{H}}_{e,0} + i\gamma/2)^{-1}\mathbf{V}_0^\dagger$ is the photon self-energy due to its coupling to the $\tilde{\mathbf{H}}_{e,0}$ block; here $\gamma \rightarrow 0$ is introduced to ensure causality of the Green’s function [30]. We next obtain an expression for $\Sigma_{e,0}(\omega)$ in terms of the bare Green’s functions and the off-diagonal light-matter couplings in Eq. 2. By iterating the technique used to obtain Eq. 4 [Supplemental material: Sec. S4], we arrive at a recursive relation where the self-energy at the k^{th} step depends on the $(k+1)^{\text{th}}$ step [27, 28]:

$$\Sigma_{e,k} = \mathbf{V}_k(\omega - \mathbf{H}_{e,k} + i\gamma/2 - \Sigma_{\text{ph},k+1})^{-1}\mathbf{V}_k^\dagger, \quad (5a)$$

$$\Sigma_{\text{ph},k+1} = \mathbf{v}_k(\omega - \mathbf{H}_{\text{ph},k+1} + i\kappa/2 - \Sigma_{e,k+1})^{-1}\mathbf{v}_k^\dagger, \quad (5b)$$

for $0 \leq k < N$. For finite N , the series truncates at $\Sigma_{\text{ph},N} = \mathbf{v}_{N-1}(\omega - \mathbf{H}_{\text{ph},N} + i\kappa/2)^{-1}\mathbf{v}_{N-1}^\dagger$. Thus Eq. 4 becomes,

$$D_N^R(\omega) = \frac{1}{\omega - \omega_{\text{ph}} + i\kappa/2 - \mathbf{V}_0 \frac{1}{\omega - \mathbf{H}_{e,0} + i\gamma/2 - \mathbf{v}_0^\dagger \frac{1}{\omega - \mathbf{H}_{\text{ph},1} + i\kappa/2 - \mathbf{v}_1^\dagger \frac{1}{\omega - \mathbf{H}_{\text{ph},2} + i\kappa/2 - \mathbf{v}_2^\dagger \frac{1}{\omega - \mathbf{H}_{\text{ph},3} + i\kappa/2 - \mathbf{v}_3^\dagger \frac{1}{\omega - \mathbf{H}_{\text{ph},N-1} + i\gamma/2 - \mathbf{v}_{N-1}^\dagger \frac{1}{\omega - \mathbf{H}_{\text{ph},N} + i\kappa/2} \mathbf{v}_N} \mathbf{v}_0} \mathbf{V}_0^\dagger}}}. \quad (6)$$

1/N expansion.—Eq. 6 admits a 1/N expansion due to the aforementioned timescale separation in the polariton dynamics, $D_N^R(\omega) = \sum_{k=0}^{\infty} d_{N,k}(\omega)$ where $d_{N,k}(\omega) \propto N^{-k}$. Here, we present closed-form expressions for $d_{N,0}$ and $d_{N,1}$. For $k \geq 2$, certain non-commuting cascade processes prevent similar analytical manipulations (Supplemental material: Sec. S6), but we can still find expressions for $d_{N,k}$ correct up to $\mathcal{O}(N^{-k})$. From Eq. 6, it is easy to see that $d_{N,0}$ must have no \mathbf{v}_n^\dagger or \mathbf{v}_n terms, so,

$$d_{N,0}(\omega) = \frac{1}{\omega - \omega_{\text{ph}} + i\kappa/2 - \mathbf{V}_0 \mathbf{G}_{e,0}(\omega) \mathbf{V}_0^\dagger}, \quad (7)$$

where $\mathbf{G}_{e,0}$ is the bare Green’s function of

$\mathbf{H}_{e,0}$ and hence $-\mathbf{V}_0 \mathbf{G}_{e,0}(\omega) \mathbf{V}_0^\dagger \equiv \frac{\omega_{\text{ph}}}{2} \chi^{(1)}(\omega) = -\lim_{\gamma \rightarrow 0^+} N \sum_{j,j'} |\lambda|^2 \frac{|\langle g, \varphi_j^{(g)} | \mu | e, \varphi_{j'}^{(e)} \rangle|^2}{\omega - (\omega_{e,j'} - \omega_{g,j}) + i\frac{\gamma}{2}}$, where $\chi^{(1)}(\omega)$ is the standard linear susceptibility of the molecular ensemble for a sample of density $N/\mathcal{V}_{\text{mol}}$ with \mathcal{V}_{mol} equal to the cavity mode volume \mathcal{V}_{ph} , and μ as the molecular transition dipole operator. The poles of $d_{N,0}(\omega)$ will hereafter be referred to as the zeroth-order polariton frequencies. In the thermodynamic limit ($N \rightarrow \infty$ or $\lambda \rightarrow 0$ while $\lambda\sqrt{N}$ is constant), $D_N^R(\omega) \approx d_{N,0}(\omega)$; so the linear response of polaritons is compactly expressed in terms of the material linear susceptibility, a result that is consistent with classical optics [9, 14, 16].

We can proceed analogously with the 1/N correction [Supplemental material: Sec. S6],

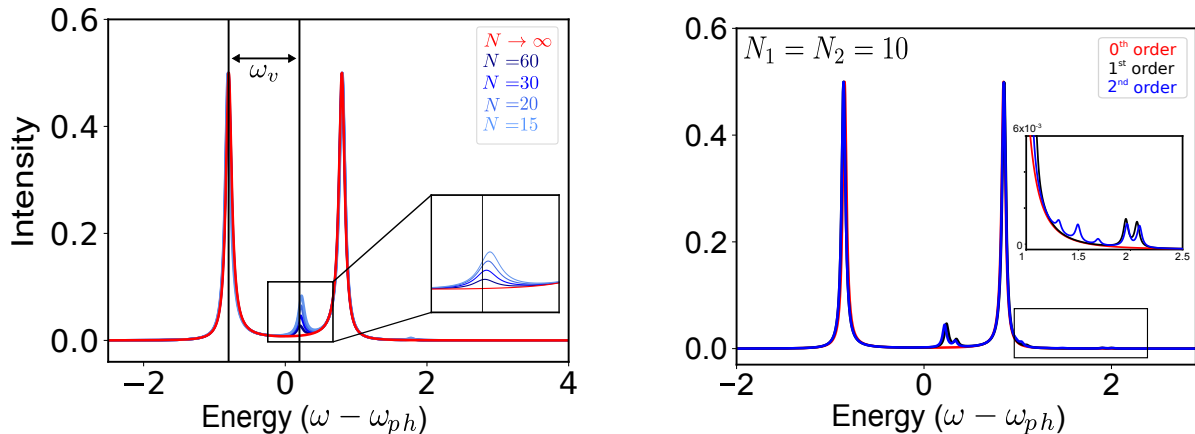


FIG. 2. (a) Linear absorption spectrum of an ensemble of 3-level systems (two ground-state vibrational levels and one excited level) at zero temperature, with fixed collective coupling $\lambda\sqrt{N}$ while varying N . The red curve is the thermodynamic limit result ($N \rightarrow \infty$) and is consistent with classical linear optics; it features resonances at the zeroth-order polaritons. First-order polariton sidebands show up at a vibrational frequency ω_v to the blue of each zeroth-order polariton and indicate Raman processes mediated by vacuum (hence, going beyond classical optics). The height of these sidebands increases as N decreases due to increasing single molecule coupling λ . Parameters: $\omega_v = 1$, $\kappa = \gamma = 0.1\omega_v$, $\lambda\sqrt{N} = 0.8\omega_v$, $\omega_{ph} = \omega_{e,0}$. (b) Linear absorption of an ensemble of two types of 3-level molecules with different vibrational gaps but the same electronic gap, including up to $\mathcal{O}(N^{-2})$ corrections. The red and black curves show zeroth- and first-order polaritons as in (a). The blue curve shows $\mathcal{O}(N^{-2})$ Raman corrections to the spectrum. Parameters: $\omega_{v,A} = 1$, $\omega_{v,B} = 1.2$, $\kappa = \gamma = 0.05\omega_v$, $\lambda\sqrt{N} = 0.6\omega_v$, $\omega_{ph} = \omega_{e,0}$ for both molecules.

$$d_{N,1}(\omega) = d_{N,0}(\omega) \cdot \mathbf{V}_0 \mathbf{G}_{e,0} \mathbf{v}_0 (\omega - \mathbf{H}_{ph,1} + i\kappa/2 - \mathbf{V}_1 \mathbf{G}_{e,1} \mathbf{V}_1^\dagger)^{-1} \mathbf{v}_0^\dagger \mathbf{G}_{e,0} \mathbf{V}_0^\dagger \cdot d_{N,0}(\omega). \quad (8)$$

In the expression, we refer to the poles of $(\omega - \mathbf{H}_{ph,1} + i\kappa/2 - \mathbf{V}_1 \mathbf{G}_{e,1} \mathbf{V}_1^\dagger)^{-1}$ as the first-order polariton frequencies, which are shifted from the zeroth-order polaritons by a Raman (vibrational) transition. Eq. 8 can be interpreted from right to left as a sequential Stokes-anti-Stokes Raman scattering process: (a) The photon entering the cavity through the zeroth-order polariton $d_{N,0}(\omega)$ carries out a Stokes Raman transition in one of the N molecules via $\mathbf{v}_0^\dagger \mathbf{G}_{e,0} \mathbf{V}_0^\dagger$, (b) the leftover Stokes photon strongly couples to the $(N - 1)$ remaining molecules forming first-order polaritons, where the Raman excited molecule serves as a spectator; (c) the first-order polariton now induces the reverse (anti-Stokes) Raman transition resetting all the molecules back to their electronic and vibrational ground state via $\mathbf{V}_0 \mathbf{G}_{e,0} \mathbf{v}_0$, while releasing the photon to the zeroth-order polariton $d_{N,0}(\omega)$. Since the creation and the annihilation of the Raman phonon are cavity vacuum-mediated, these transitions are individually penalized by $1/\sqrt{N}$ and go beyond the classical optics formalism. To understand the spectroscopic fingerprints, we present an illustrative example.

Let us consider the model in Eq. 1, with each molecule having two vibrational levels in the ground state ($|g, \varphi_0^{(g)}\rangle$, $|g, \varphi_1^{(g)}\rangle$) and one excited state ($|e, \varphi_0^{(e)}\rangle$); this simplified model is already rich enough to illus-

trate the physics of interest. The vibrational gap is $\omega_v = \omega_{\varphi_1^{(g)}} - \omega_{\varphi_0^{(g)}}$ and the cavity is resonant with the $|g, \varphi_0^{(g)}\rangle \rightarrow |e, \varphi_0^{(e)}\rangle$ transition with frequency $\omega_{e,0}$. Fig. 2a shows the $A(\omega)$ in the thermodynamic limit and the $1/N$ corrections computed using Eq. 8. As N decreases, the $1/N$ correction reveals two sidebands separated from the zeroth-order polaritons by ω_v . These first-order polaritons have a Rabi splitting of $2\lambda\sqrt{N-1}$, and they have featured in previously reported calculations of polaritonic systems where N is small [31]. The shift between the zeroth and first-order polaritons, corresponding to the energy difference of the ground state vibrational levels, provides information analogous to a Raman spectrum. A discrepancy in the Rabi splitting, $\Delta = 2\lambda(\sqrt{N} - \sqrt{N-1})$, causes a blue shift in the first-order peaks (see Fig. 2a inset), due to the decrease in $\lambda\sqrt{N-1}$ as N decreases while $\lambda\sqrt{N}$ remains constant. The blue-shift Δ scales as $1/\sqrt{N}$, and the peak height as $1/N$; this latter scaling can be understood from Eq. 8 since each action of \mathbf{v}_0 and \mathbf{v}_0^\dagger is proportional to $N^{-1/2}$.

Even though we cannot provide an expression for $d_{N,k}$ when $k \geq 2$, the truncation of Eq. 6 at $\mathbf{H}_{e,k}$ gives $D_N^R(\omega)$ up to $\mathcal{O}(N^{-k})$. To best illustrate the spectroscopic implications of the $\mathcal{O}(N^{-2})$ corrections to $d_{N,0}(\omega)$, we

consider a cavity coupled to N_A and N_B molecules of two different species. Eq. 1 can be trivially generalized to account for two sets of bosonic modes corresponding to the different molecules [32]. Each molecule is modeled as a 3-level system with different vibrational gaps, $\omega_{v,A}$ and $\omega_{v,B}$. For simplicity, let the electronic transition frequencies, $\omega_{e,\varphi_{0,i}^{(e)}} - \omega_{g,\varphi_{0,i}^{(g)}}$, is identical for both species $i = A, B$. Fig. 2b shows $A(\omega)$ for this setup. Including the second-order correction introduces sidebands shifted from the zeroth-order polaritons by

$$D_N^R(\omega) = \frac{1}{\omega - \omega_{\text{ph}} + i\kappa/2 + \sum_{l=0}^{\infty} \left(\frac{\omega_{\text{ph}}}{2}\right)^l \chi_N^{(2l+1)}(\{\omega, \omega - \omega_{\text{ph}}\}^l, \omega)}, \quad (9)$$

where $\sum_{l=0}^{\infty} \left(\frac{\omega_{\text{ph}}}{2}\right)^l \chi_N^{(2l+1)}(\{\omega, \omega - \omega_{\text{ph}}\}^l, \omega)$ is the sum over all the *irreducible* Rayleigh and Raman nonlinear susceptibilities of the N -molecule ensemble ($\{\omega, \omega - \omega_{\text{ph}}\}^l$ denotes a string where $\omega, \omega - \omega_{\text{ph}}$ are repeated l times). We shall now define the concept of *reducible* (*irreducible*) nonlinear susceptibilities, which describe processes that can (cannot) be decomposed into products of other bare susceptibilities, $\chi_N^{2l+1}(\sum_{i=1}^{2l+1} \omega_i, \dots, \omega_1)$ [30, 35]; as far as we aware, this concept does not exist in the literature, although similar ideas are standard in diagrammatic many-body theory [36]. The key difference between *reducible* and *irreducible* susceptibilities lies in whether, upon initial excitation of molecules via \mathbf{V}_0^\dagger , the excitation fully returns to the cavity mode via \mathbf{V}_0 at an intermediate step or not; see Fig. 3. It is easy to see that the expansion of the self-energy in Eq. 6 into terms of different order in light-matter coupling gives rise to irreducible diagrams only (\mathbf{V}_0 and \mathbf{V}_0^\dagger act only at the beginning and end). Another interesting observation is that interpreting Eq. 9 as a geometric series gives rise to all the possible *reducible* and irreducible diagrams for cavity linear response.

Experimental considerations.—The spectral resolution of the polaritonic linear response is mainly determined by its cavity lifetime, $2\pi/\kappa$. Given that the peak heights correspond to the vacuum-induced nonlinearities determined by the single-molecule light-matter coupling λ , κ must be comparable to λ to resolve these features. This insight also helps understand why, in typical experiments with low-Q cavities, $\kappa \gg \lambda$, the truncation of the $1/N$ expansion at $d_{N,0}$ works so well. Another reason why these nonlinearities are not typically observed is due to the use of multimode cavities, given that the here-predicted first-order polariton peaks will instead blur into broad continua (the Stokes Raman photon can be emitted into any cavity mode)[37]. Thus,

$2\omega_{g,A}$, $2\omega_{g,B}$, and $\omega_{g,A} + \omega_{g,B}$ (see the three peaks appearing only in blue in the inset) due to a Raman process involving the second-order polaritons. These shifts correspond to the sum of Raman transition frequencies created in two molecules of the same or different species, in a similar way that entangled photons induce collective resonances between different molecules [33, 34].

Feynman pathways.—For simplicity, we return to the discussion of an ensemble of identical molecules. It turns out that Eq. 6 can be rewritten as [Supplemental Material: Sec. S5],

effective single-mode cavities are needed, which, from an experimental standpoint, translate into cavities with large free spectral ranges or with dispersionless cavities. [38–41].

Summary and conclusions.—We demonstrated that while the thermodynamic limit of molecular polaritons in typical Fabry-Perot cavities, with broad linewidths, is well-captured by classical linear optics, high-Q, single-mode cavities can reveal the otherwise hidden nonlinearities expected in systems under SC. To capture these effects, we derived a general expression for the linear response of polaritons beyond the classical regime, expressed in terms of *irreducible* Rayleigh and Raman nonlinear susceptibilities of the molecular ensemble. By leveraging the timescale hierarchy in the polariton problem, we presented a $1/N$ expansion of this expression. While we focused on the spectroscopic aspects of the problem, we believe these higher-order coherent processes in the molecular ensemble could serve as a pathway for harnessing quantum resources such as entanglement and nontrivial photon statistics, which will be explored in future works.

A.K. thanks Sricharan Raghavan-Chitra, Juan B. Pérez-Sánchez, Piper Fowler-Wright, Juan Carlos Obeso Jureidini, and Kai Schwennicke for useful discussions. J.Y.Z. and A.K. thank Abraham Nitzan for providing the connection with Raman and Rayleigh scattering and for asking whether the result holds for multimode cavities.

* joelyuen@ucsd.edu

[1] D. M. Coles, N. Somaschi, P. Michetti, C. Clark, P. G. Lagoudakis, P. G. Savvidis, and D. G. Lidzey, “Polariton-mediated energy transfer between organic dyes in a

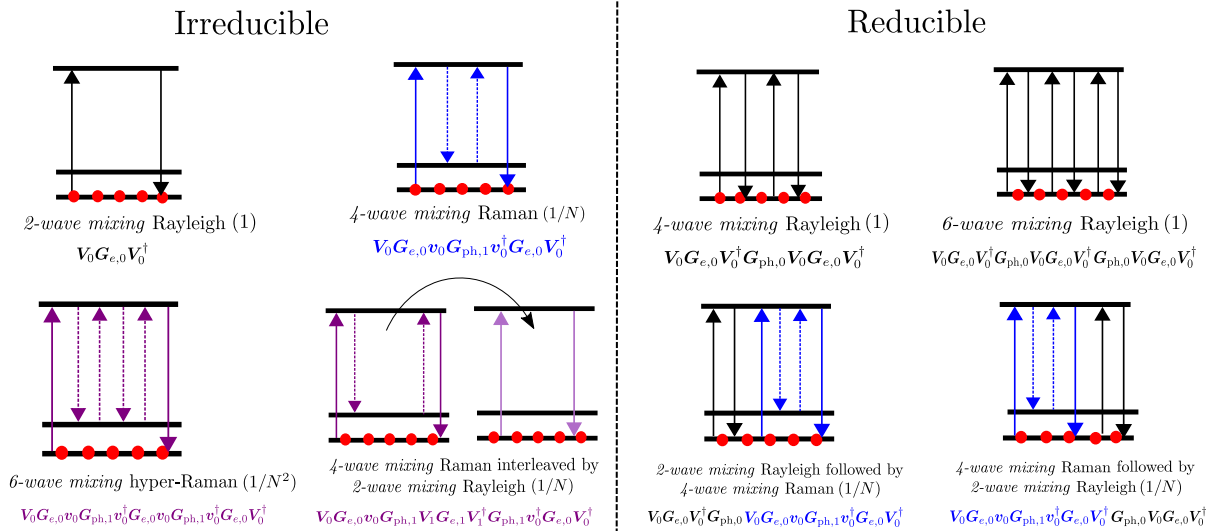


FIG. 3. *Cavity-mediated nonlinear molecular processes*: Ladder diagrams for an ensemble of identical three-level systems with two ground-state vibrational levels and one excited state, showing second, fourth, and sixth-order transitions mediated by the cavity, classified into *reducible* and *irreducible* nonlinear susceptibilities with their correction order in the parentheses. The **second-order** term represents a *2-wave mixing* collective Rayleigh process. The **fourth-order** term includes two contributions: a collective *4-wave mixing* Rayleigh and a *4-wave mixing* Raman. The **sixth-order** term has five contributions: a collective *6-wave mixing* Rayleigh, two *reducible* terms involving *2-wave mixing* Rayleigh and *4-wave mixing* Raman, a *6-wave mixing* Raman, and a cascade process involving two molecules with a *4-wave mixing* Raman interleaved by a *2-wave mixing* Rayleigh. The distinction between *reducible* and *irreducible* contributions lies in whether the excitation, after the initial V_0 interaction with the molecular ensemble, fully returns to $H_{ph,0}$ ($G_{ph,0}$) via the V_0^\dagger interaction at any intermediate step.

- strongly coupled optical microcavity,” *Nature Materials* **13**, 712–719 (2014).
- [2] M. Reitz, F. Mineo, and C. Genes, “Energy transfer and correlations in cavity-embedded donor-acceptor configurations,” *Scientific Reports* **8**, 9050 (2018).
- [3] A. Koner, M. Du, S. Pannir-Sivajothi, R. H. Goldsmith, and J. Yuen-Zhou, “A path towards single molecule vibrational strong coupling in a fabry-pérot microcavity,” *Chemical Science* **14**, 7753–7761 (2023).
- [4] J. A. Hutchison, T. Schwartz, C. Genet, E. Devaux, and T. W. Ebbesen, “Modifying chemical landscapes by coupling to vacuum fields,” *Angewandte Chemie International Edition* **51**, 1592–1596 (2012).
- [5] F. Herrera and J. Owrutsky, “Molecular polaritons for controlling chemistry with quantum optics,” *The Journal of Chemical Physics* **152** (2020).
- [6] F. Freire-Fernández, N. G. Sinai, M. J. Hui Tan, S.-M. Park, E. R. Koessler, T. Krauss, P. Huo, and T. W. Odom, “Room-temperature polariton lasing from cds core-only nanoplatelets,” *ACS Nano* **18**, 15177–15184 (2024).
- [7] C. Bennenhei, M. Struve, S. Stephan, N. Kunte, V. N. Mitryakhin, F. Eilenberger, J. Ohmer, U. Fischer, M. Silies, C. Schneider, and M. Esmann, “Polarized room-temperature polariton lasing in elliptical microcavities filled with fluorescent proteins,” *Opt. Mater. Express* **13**, 2633–2643 (2023).
- [8] K. S. Daskalakis, S. A. Maier, and S. Kéna-Cohen, “Polariton condensation in organic semiconductors,” *Quantum Plasmonics*, 151–163 (2017).
- [9] K. Schwennicke, A. Koner, J. B. Pérez-Sánchez, W. Xiong, N. C. Giebink, M. L. Weichman, and J. Yuen-Zhou, “When do molecular polaritons behave like optical filters?” (2024), arXiv:2408.05036 [physics.chem-ph].
- [10] Y. Zhu, D. J. Gauthier, S. Morin, Q. Wu, H. Carmichael, and T. Mossberg, “Vacuum rabi splitting as a feature of linear-dispersion theory: Analysis and experimental observations,” *Physical Review Letters* **64**, 2499 (1990).
- [11] M. Schubert, “Polarization-dependent optical parameters of arbitrarily anisotropic homogeneous layered systems,” *Physical Review B* **53**, 4265 (1996).
- [12] A. Yariv and P. Yeh, *Photonics: optical electronics in modern communications* (Oxford University Press, 2007).
- [13] N. Német, D. White, S. Kato, S. Parkins, and T. Aoki, “Transfer-matrix approach to determining the linear response of all-fiber networks of cavity-qed systems,” *Physical Review Applied* **13**, 064010 (2020).
- [14] J. A. Ćwik, P. Kirton, S. De Liberato, and J. Keeling, “Excitonic spectral features in strongly coupled organic polaritons,” *Physical Review A* **93**, 033840 (2016).
- [15] S. Gunasekaran, R. F. Pinar, and A. J. Musser, “Continuum model of strong light-matter coupling for molecular polaritons,” arXiv preprint arXiv:2308.08744 (2023).
- [16] J. Yuen-Zhou and A. Koner, “Linear response of molecular polaritons,” *The Journal of Chemical Physics* **160**, 154107 (2024).
- [17] J. B. Pérez-Sánchez and J. Yuen-Zhou, “Radiative pumping vs vibrational relaxation of molecular polaritons: a bosonic mapping approach,” (2024), arXiv:2407.20594 [quant-ph].
- [18] M. Gegg and M. Richter, “Efficient and exact numerical approach for many multi-level systems in open system cqed,” *New J. Phys.* **18**, 043037 (2016).

- [19] N. Shammah, S. Ahmed, N. Lambert, S. De Liberato, and F. Nori, “Open quantum systems with local and collective incoherent processes: Efficient numerical simulations using permutational invariance,” *Phys. Rev. A* **98**, 063815 (2018).
- [20] M. A. Zeb, “Efficient linear scaling mapping for permutation symmetric fock spaces,” *Comp. Phys. Commun.* **276**, 108347 (2022).
- [21] R. E. F. Silva and J. Feist, “Permutational symmetry for identical multilevel systems: A second-quantized approach,” *Phys. Rev. A* **105**, 043704 (2022).
- [22] V. Sukharnikov, S. Chuchurka, A. Benediktovitch, and N. Rohringer, “Second quantization of open quantum systems in liouville space,” *Phys. Rev. A* **107**, 053707 (2023).
- [23] J. B. Pérez-Sánchez, A. Koner, S. Raghavan-Chitra, and J. Yuen-Zhou, “Cut- e as a $1/n$ expansion for multiscale molecular polariton dynamics,” (2024), arXiv:2410.14175 [quant-ph].
- [24] M. R. Philpott, “Theory of the Coupling of Electronic and Vibrational Excitations in Molecular Crystals and Helical Polymers,” *J. Chem. Phys.* **55**, 2039–2054 (1971).
- [25] F. Herrera and F. C. Spano, “Dark vibronic polaritons and the spectroscopy of organic microcavities,” *Phys. Rev. Lett.* **118**, 223601 (2017).
- [26] J. B. Pérez-Sánchez, A. Koner, N. P. Stern, and J. Yuen-Zhou, “Simulating molecular polaritons in the collective regime using few-molecule models,” *Proceedings of the National Academy of Sciences* **120**, e2219223120 (2023).
- [27] J. Velev and W. Butler, “On the equivalence of different techniques for evaluating the green function for a semi-infinite system using a localized basis,” *Journal of Physics: Condensed Matter* **16**, R637 (2004).
- [28] H. M. Pastawski, J. F. Weisz, and S. Albornoz, “Matrix continued-fraction calculation of localization length,” *Phys. Rev. B* **28**, 6896–6903 (1983).
- [29] P. Hänggi, F. Rösel, and D. Trautmann, “Continued fraction expansions in scattering theory and statistical nonequilibrium mechanics,” *Zeitschrift für Naturforschung A* **33**, 402–417 (1978).
- [30] S. Mukamel, *Principles of nonlinear optical spectroscopy* (Oxford University Press, 1995).
- [31] M. A. Zeb, P. G. Kirton, and J. Keeling, “Exact states and spectra of vibrationally dressed polaritons,” *ACS Photonics* **5**, 249–257 (2018).
- [32] J. B. Pérez-Sánchez, F. Mellini, N. C. Giebink, and J. Yuen-Zhou, “Frequency-dependent photoreactivity in disordered molecular polaritons,” arXiv preprint arXiv:2308.03954 (2023).
- [33] A. Muthukrishnan, G. S. Agarwal, and M. O. Scully, “Inducing disallowed two-atom transitions with temporally entangled photons,” *Phys. Rev. Lett.* **93**, 093002 (2004).
- [34] T. Seidelmann, C. Schimpf, T. K. Bracht, M. Cosacchi, A. Vagov, A. Rastelli, D. E. Reiter, and V. M. Axt, “Two-photon excitation sets limit to entangled photon pair generation from quantum emitters,” *Phys. Rev. Lett.* **129**, 193604 (2022).
- [35] R. Glenn, K. Bennett, K. E. Dorfman, and S. Mukamel, “Photon-exchange induces optical nonlinearities in harmonic systems,” *Journal of Physics B: Atomic, Molecular and Optical Physics* **48**, 065401 (2015).
- [36] A. Fetter and J. Walecka, *Quantum Theory of Many-particle Systems*, Dover Books on Physics (Dover Publications, 2003).
- [37] G. Engelhardt and J. Cao, “Polariton localization and dispersion properties of disordered quantum emitters in multimode microcavities,” *Phys. Rev. Lett.* **130**, 213602 (2023).
- [38] C.-h. Xue, Y. Ding, H.-t. Jiang, Y. Li, Z.-s. Wang, Y.-w. Zhang, and H. Chen, “Dispersionless gaps and cavity modes in photonic crystals containing hyperbolic metamaterials,” *Phys. Rev. B* **93**, 125310 (2016).
- [39] S. Fujii and T. Tanabe, “Dispersion engineering and measurement of whispering gallery mode microresonator for kerr frequency comb generation,” *Nanophotonics* **9**, 1087–1104 (2020).
- [40] Y. A. García Jomaso, B. Vargas, D. L. Domínguez, R. J. Armenta-Rico, H. E. Saucedo, C. L. Ordoñez-Romero, H. A. Lara-García, A. Camacho-Guardian, and G. Pirruccio, “Intercavity polariton slows down dynamics in strongly coupled cavities,” *Nature Communications* **15**, 2915 (2024).
- [41] F. Baboux, L. Ge, T. Jacqmin, M. Biondi, E. Galopin, A. Lemaître, L. Le Gratiet, I. Sagnes, S. Schmidt, H. E. Türeci, A. Amo, and J. Bloch, “Bosonic condensation and disorder-induced localization in a flat band,” *Phys. Rev. Lett.* **116**, 066402 (2016).

Hidden nonlinear optical susceptibilities in linear polaritonic spectra: Supplemental material

Arghadip Koner¹ and Joel Yuen-Zhou^{1,*}

¹*Department of Chemistry and Biochemistry, University of California San Diego, La Jolla, California 92093*

(Dated: November 19, 2024)

S1. THE HAMILTONIAN

The SC setup consisting of a photonic cavity with a single mode of frequency ω_{ph} coupled to N non-interacting molecules is typically modeled using the Holstein-Tavis-Cummings Hamiltonian extended to arbitrary vibronic structures [1],

$$H_{HTC} = \hbar\omega_{\text{ph}}a^\dagger a + \sum_{i=1}^N \left(\hat{T}_i + V_g(q_i)|g_i\rangle\langle g_i| + V_e(q_i)|e_i\rangle\langle e_i| \right) + \hbar\lambda \sum_i^N (|e_i\rangle\langle g_i|a + |g_i\rangle\langle e_i|a^\dagger), \quad (\text{S.1})$$

where \hat{T} is the kinetic energy operator, $V_{g/e}$ are the ground/excited potential energy surfaces (PES), $\hbar\lambda$ is the single-molecule light-matter coupling strength, and a is the annihilation operator of a photon in the cavity mode. Pérez-Sánchez *et. al.* has shown that starting from a permutationally invariant initial state and exploiting the symmetries under the permutations of the molecules, the setup obeys a second-quantized bosonic Hamiltonian [1–4],

$$H = H_0 + V = \left[\hbar\omega_{\text{ph}}a^\dagger a + \hbar \sum_{j=1}^{M_g} \omega_{g,j} b_j^\dagger b_j + \hbar \sum_{j=1}^{M_e} \omega_{e,j} B_j^\dagger B_j \right] + \left[-\hbar\lambda \sum_{jj'} \langle \varphi_{j'}^{(e)} | \varphi_j^{(g)} \rangle a b_j B_{j'}^\dagger - \text{h.c.} \right]. \quad (\text{S.2})$$

Here, H_0 represents the zeroth-order contribution from the bare cavity and the molecules, and V models the cavity-molecule interaction with coupling strength $\hbar\lambda$. The operators b_j and $B_{j'}$ annihilate a molecule in a vibronic state $|g, \varphi_j^{(g)}\rangle$ (the first and the second index represents the electronic state and the vibrational states, respectively), and a molecule in the vibronic state $|e, \varphi_{j'}^{(e)}\rangle$, respectively. The eigenstates of the non-interacting part of the Hamiltonian, H^0 , are represented as $|n_{\text{ph}}; n_1, n_2, \dots, n_{M_g}; n'_1, n'_2, \dots, n'_{M_e}\rangle$, where M_g and M_e are the sizes of the vibrational bases used in the model, n_i (n'_i) is the number of molecules in the i^{th} vibrational level of the ground (excited) electronic state, and n_{ph} is the number of photonic excitations [5, 6]. In the rest of this work, we will consider our initial state to be $|0; N, \vec{0}; \vec{0}\rangle$, which is a photonless state with all the molecules in the global ground state (zero temperature). Although the bosonic picture is valid for an arbitrary number of excitations in the system, the linear response regime restricts us to the first excitation manifold in the Hamiltonian. We have previously shown in Ref. [1] that in the eigenbasis of H_0 , H admits a block tridiagonal representation:

$$H_1 = \begin{pmatrix} \mathbf{H}_{\text{ph},0} & \mathbf{V}_0 & 0 & \dots & 0 & 0 & 0 \\ \mathbf{V}_0^\dagger & \mathbf{H}_{e,0} & \mathbf{v}_0 & \dots & 0 & 0 & 0 \\ 0 & \mathbf{v}_0^\dagger & \mathbf{H}_{\text{ph},1} & \mathbf{V}_1 & 0 & 0 & 0 \\ \vdots & \vdots & \vdots & \ddots & \vdots & \vdots & \vdots \\ 0 & 0 & 0 & \dots & \mathbf{V}_{N-1}^\dagger & \mathbf{H}_{e,N-1} & \mathbf{v}_{N-1} \\ \vdots & \vdots & \vdots & \vdots & 0 & \mathbf{v}_{N-1}^\dagger & \mathbf{H}_{\text{ph},N} \end{pmatrix} \quad (\text{S.3})$$

* joelyuen@ucsd.edu

The sub-blocks of H_1 of the form $\begin{pmatrix} \mathbf{H}_{\text{ph},n} & \mathbf{V}_n \\ \mathbf{V}_n^\dagger & \mathbf{H}_{e,n} \end{pmatrix}$ have n , the number of molecules with electronic ground state (GS) phonons as a conserved quantity, and only the slow $\mathbf{v}_n \propto \lambda$ interactions can change the number of molecules with electronic GS phonons, leading to a timescale separation in the quantum dynamics. The block tridiagonal structure of H_1 allows for its representation as a nearest neighbor coupled chain model [7–14],

$$\boxed{\mathbf{H}_{\text{ph},0} \begin{matrix} \leftarrow \mathbf{V}_0^\dagger \\ \mathbf{V}_0 \end{matrix} \mathbf{H}_{e,0}} \begin{matrix} \leftarrow \mathbf{v}_0^\dagger \\ \mathbf{v}_0 \end{matrix} \boxed{\mathbf{H}_{\text{ph},1} \begin{matrix} \leftarrow \mathbf{V}_1^\dagger \\ \mathbf{V}_1 \end{matrix} \mathbf{H}_{e,1}} \begin{matrix} \leftarrow \mathbf{v}_1^\dagger \\ \mathbf{v}_1 \end{matrix} \dots \boxed{\mathbf{H}_{\text{ph},N-1} \begin{matrix} \leftarrow \mathbf{V}_{N-1}^\dagger \\ \mathbf{V}_{N-1} \end{matrix} \mathbf{H}_{e,N-1}} \begin{matrix} \leftarrow \mathbf{v}_N^\dagger \\ \mathbf{v}_N \end{matrix} \mathbf{H}_{\text{ph},N}. \quad (\text{S.4})$$

We call this the CUT-E (collective dynamics using truncated equations) diagram, based on Ref. [15], where this timescale separation was first formulated. We will use it to develop a diagrammatic approach later.

S2. THE PHOTON GREEN'S FUNCTION

The linear spectroscopic observables for the polaritonic setup with N molecules are functions of the photon Green's function, $D_N^R(\omega) = -i \int_{-\infty}^{\infty} dt e^{i\omega t} \Theta(t) \langle [a(t), a^\dagger] \rangle$ [16, 17]; the average $\langle \dots \rangle$ is computed with respect to the initial state. We have the transmission, $T(\omega)$, absorption, $A(\omega)$, and reflection, $R(\omega)$,

$$T(\omega) = (\kappa^2/4) |D_N^R(\omega)|^2, \quad (\text{S.5a})$$

$$R(\omega) = 1 + \kappa \text{Im} D_N^R(\omega) + (\kappa^2/4) |D_N^R(\omega)|^2, \quad (\text{S.5b})$$

$$A(\omega) = -(\kappa/2) [\kappa |D_N^R(\omega)|^2 + 2 \text{Im} D_N^R(\omega)]. \quad (\text{S.5c})$$

For our zero-temperature ($\mathcal{T} = 0$) photonless initial state, we can eliminate one of the terms in the commutator, giving

$$D_N^R(\omega)|_{\mathcal{T}=0} = -i \int_{-\infty}^{\infty} dt e^{i\omega t} \Theta(t) \langle a e^{-iHt} a^\dagger \rangle \quad (\text{S.6})$$

$$= \langle a G(\omega) a^\dagger \rangle, \quad (\text{S.7})$$

where $G(\omega) = -i \int_{-\infty}^{\infty} dt e^{i\omega t} \Theta(t) e^{-iHt} = \frac{1}{\omega - H + i0^+}$ is the full system's Green's function. Now to compute $D_N^R(\omega)$, we can use the Dyson series,

$$\begin{aligned} G &= G_0 + G_0 V G \\ &= G_0 + G_0 V G_0 + G_0 V G_0 V G_0 + \dots \end{aligned} \quad (\text{S.8})$$

where $G_0 = \frac{1}{\omega - H_0 + i0^+}$ is the Green's function of the noninteracting part. Typically double-sided Feynmann diagrams (DS-FDs) [18] are used in the theory of nonlinear spectroscopy to compute the terms in the Dyson series. **However, notice that elimination of one of the terms of the commutator at $\mathcal{T} = 0$ implies that exclusively the *ket*-only DS-FDs have non-zero contributions to $D_N^R(\omega)$.** The physical implication of this result is that only optical coherences contribute to the response in the linear regime, a result that is also consistent with the understanding of linear response outside of cavities. In Fig S1, we show the *ket*-only diagrams up to the fourth order. Notice that only the terms, even orders in V , contribute to a non-zero response. This is a consequence of the fact that the interaction V can only exchange the excitation between the cavity and the molecules.

The result that only *ket*-only diagrams contribute allows us to use the CUT-E diagram instead of the DS-FDs to compute the different orders in the Dyson series. In addition to the notational simplicity, the CUT-E diagram separates the nonlinear transitions based on their timescales. This will later help us obtain the $1/N$ expansion. Here, we state the rules for using the CUT-E diagram to compute the terms of the Dyson series:

1. The $(2m)^{\text{th}}$ order term in $D_N^R(\omega)$ consists of all the $2m$ step paths in the CUT-E diagram *starting from* and *returning* to $\mathbf{H}_{\text{ph},0}$; the order here is calculated with respect to the light-matter interaction, V ,
2. Every time we jump from one box to another in the CUT-E diagram, we encounter a Raman process mediated by a $\mathbf{v}_k^{(\dagger)}$ which are penalized by a factor of $1/\sqrt{N}$.

It can be seen (and proven explicitly using mathematical induction) that the CUT-E diagram with the aforementioned

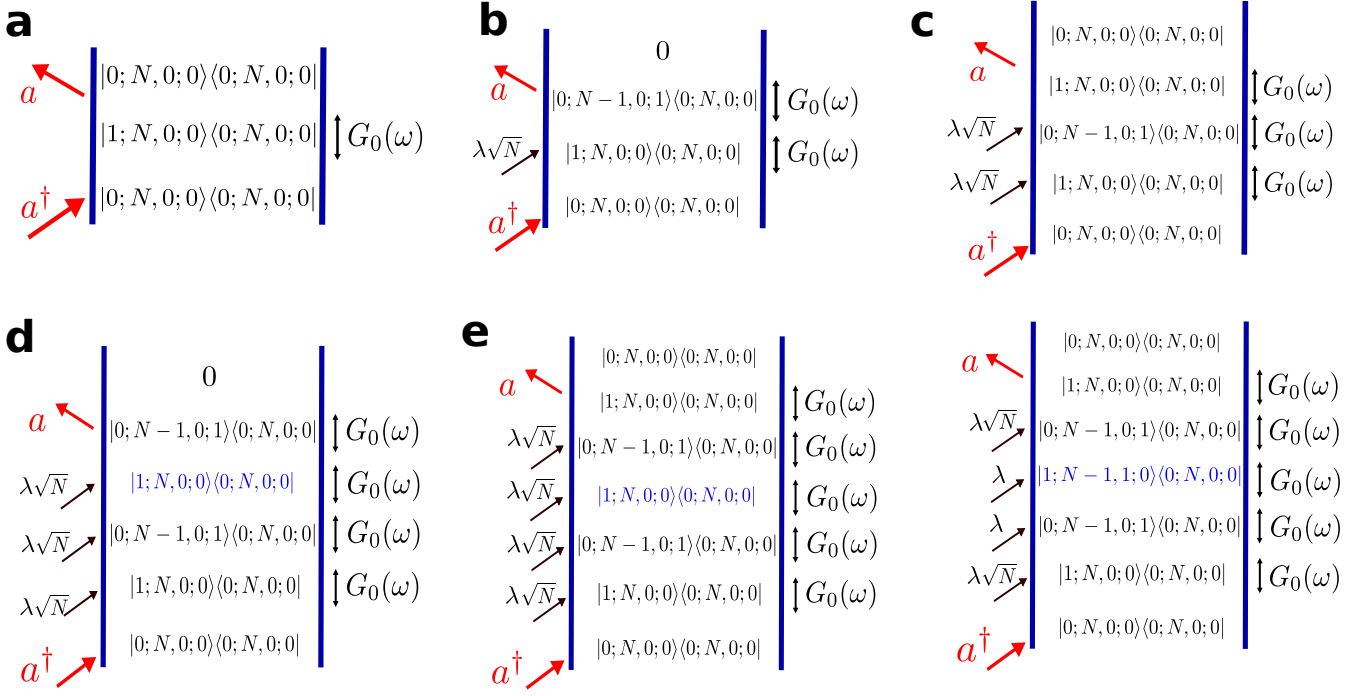


Figure S1: The *ket*-only DS-FDs for the a. zeroth, b. first, c. second, d. third, and e. fourth order. Notice that only the even orders have non-zero contributions. It can be checked that for the $\mathcal{T} = 0$ photonless initial state, at a given order, these are the only diagrams that contribute. In the fourth order, we notice that the second diagram involving a Raman process is penalized by a factor of $1/N$.

rules is equivalent to computing *ket*-only diagrams. Below, we will show a few examples of using the CUT-E diagram to compute the terms of $D^R(\omega)$ at different orders of the Dyson series with the k^{th} order term denoted as $D^{R,(k)}(\omega)$.

1. **Zeroth order term:** 0 step paths. We have $D^{R,(0)}(\omega) = \mathbf{G}_{\text{ph},0}(\omega) = \frac{1}{\omega - \omega_{\text{ph}} + i\kappa/2}$.

2. **Second order term:** We want to count the 2 step paths. We have just one of them: $\boxed{\mathbf{H}_{\text{ph},0} \overset{1}{\leftarrow} \overset{2}{\leftarrow} \mathbf{H}_{e,0}}$ (the numbers on the top (bottom) represent the counting of the step forward (backward)). Thus, second-order photon Green's function, $D^{R,(2)}(\omega)$, is then given as

$$D^{R,(2)}(\omega) = \mathbf{G}_{\text{ph},0}(\mathbf{V}_0 \mathbf{G}_{e,0} \mathbf{V}_0^\dagger) \mathbf{G}_{\text{ph},0}, \quad (\text{S.9})$$

3. **Fourth order term:** All the 4 step paths are presented in the table below. The fourth-order photon Green's function, $D^{R,(4)}(\omega)$, is then given as the sum of all the Dyson series terms,

$D_N^{R,(4)}(\omega)$	Pathways in CUT-E diagram	Dyson series term
	$\mathbf{H}_{\text{ph},0} \overset{1,3}{\leftarrow} \overset{2,4}{\leftarrow} \mathbf{H}_{e,0} = 2 \cdot (\mathbf{H}_{\text{ph},0} \leftrightarrow \mathbf{H}_{e,0})$	$\mathbf{G}_{\text{ph},0} \cdot (\mathbf{V}_0 \mathbf{G}_{e,0} \mathbf{V}_0^\dagger \mathbf{G}_{\text{ph},0})^2$
	$\mathbf{H}_{\text{ph},0} \overset{1}{\leftarrow} \mathbf{H}_{e,0} \overset{2}{\leftarrow} \mathbf{H}_{\text{ph},1}$	$\mathbf{G}_{\text{ph},0} (\mathbf{V}_0 \mathbf{G}_{e,0} \mathbf{v}_0 \mathbf{G}_{\text{ph},1} \mathbf{v}_0^\dagger \mathbf{G}_{e,0} \mathbf{V}_0^\dagger) \mathbf{G}_{\text{ph},0}$

4. **Sixth order term:** We want all the 6-step paths in the diagram. We can have five of them presented in the table below. Note that $D_N^{R,(6)}(\omega)$ is the sum of all the Dyson series terms.

$D_N^{R,(6)}(\omega)$	Pathways in CUT-E diagram	Dyson series term
	$\mathbf{H}_{\text{ph},0} \xleftrightarrow[2,4,6]{1,3,5} \mathbf{H}_{e,0} = 3 \cdot (\mathbf{H}_{\text{ph},0} \leftrightarrow \mathbf{H}_{e,0})$	$\mathbf{G}_{\text{ph},0} \left(\mathbf{V}_0 \mathbf{G}_{e,0} \mathbf{V}_0^\dagger \mathbf{G}_{\text{ph},0} \right)^3$
	$\mathbf{H}_{\text{ph},0} \xleftrightarrow[2,6]{1,3} \mathbf{H}_{e,0} \xleftrightarrow[5]{4} \mathbf{H}_{\text{ph},1}$	$\mathbf{G}_{\text{ph},0} (\mathbf{V}_0 \mathbf{G}_{e,0} \mathbf{V}_0^\dagger) \mathbf{G}_{\text{ph},0} (\mathbf{V}_0 \mathbf{G}_{e,0} \mathbf{v}_0 \mathbf{G}_{\text{ph},1} \mathbf{v}_0^\dagger \mathbf{G}_{e,0} \mathbf{V}_0^\dagger) \mathbf{G}_{\text{ph},0}$
	$\mathbf{H}_{\text{ph},0} \xleftrightarrow[4,6]{1,5} \mathbf{H}_{e,0} \xleftrightarrow[3]{2} \mathbf{H}_{\text{ph},1}$	$\mathbf{G}_{\text{ph},0} (\mathbf{V}_0 \mathbf{G}_{e,0} \mathbf{v}_0 \mathbf{G}_{\text{ph},1} \mathbf{v}_0^\dagger \mathbf{G}_{e,0} \mathbf{V}_0^\dagger) \mathbf{G}_{\text{ph},0} (\mathbf{V}_0 \mathbf{G}_{e,0} \mathbf{V}_0^\dagger) \mathbf{G}_{\text{ph},0}$
	$\mathbf{H}_{\text{ph},0} \xleftrightarrow[6]{1} \mathbf{H}_{e,0} \xleftrightarrow[3,5]{2,4} \mathbf{H}_{\text{ph},1}$	$\mathbf{G}_{\text{ph},0} (\mathbf{V}_0 \mathbf{G}_{e,0} \mathbf{v}_0 \mathbf{G}_{\text{ph},1} \mathbf{v}_0^\dagger \mathbf{G}_{e,0} \mathbf{v}_0 \mathbf{G}_{\text{ph},1} \mathbf{v}_0^\dagger \mathbf{G}_{e,0} \mathbf{V}_0^\dagger) \mathbf{G}_{\text{ph},0}$
	$\mathbf{H}_{\text{ph},0} \xleftrightarrow[6]{1} \mathbf{H}_{e,0} \xleftrightarrow[5]{2} \mathbf{H}_{\text{ph},1} \xleftrightarrow[4]{3} \mathbf{H}_{e,0}$	$\mathbf{G}_{\text{ph},0} (\mathbf{V}_0 \mathbf{G}_{e,0} \mathbf{v}_0 \mathbf{G}_{\text{ph},1} \mathbf{V}_1 \mathbf{G}_{e,1} \mathbf{V}_1^\dagger \mathbf{G}_{\text{ph},1} \mathbf{v}_0^\dagger \mathbf{G}_{e,0} \mathbf{V}_0^\dagger) \mathbf{G}_{\text{ph},0}$

We will come to these results in Sec. S5 where we discuss *reducible* and *irreducible* diagrams.

S3. SOME RESULTS FOR MATRIX GREEN'S FUNCTION AND MATRICES

This section is quite standard but is presented for completeness and for pedagogical purposes. [8, 9, 19].

A. Green's function of two connected systems

Let us first consider two uncoupled systems, A and B with their bare Green's functions G_{AA}^0 and G_{BB}^0 , respectively. If these systems are coupled by an interaction $V = V_{AB} + V_{BA}$,

$$G = (E - H_0 - V)^{-1} = ((G_0)^{-1} - V)^{-1}.$$

Explicitly,

$$G = \begin{pmatrix} (G_{AA}^0)^{-1} & -V_{AB} \\ -V_{BA} & (G_{BB}^0)^{-1} \end{pmatrix}^{-1}.$$

To find the inverse, we will use the method of Schur complement (see sec. S3B). We have

$$\begin{aligned} G_{AA} &= ((G_{AA}^0)^{-1} - V_{AB} G_{BB}^0 V_{BA})^{-1}, \\ G_{BB} &= ((G_{BB}^0)^{-1} - V_{BA} G_{AA}^0 V_{AB})^{-1}, \\ G_{AB} &= -G_{AA}^0 (-V_{AB}) ((G_{BB}^0)^{-1} - V_{BA} G_{AA}^0 V_{AB})^{-1} \\ &= G_{AA}^0 V_{AB} G_{BB}, \\ G_{BA} &= G_{BB}^0 V_{BA} G_{AA}. \end{aligned}$$

B. Schur complement

Let A, B, C, D be $p \times p, p \times q, q \times p$ and $q \times q$ matrices of complex numbers. and construct,

$$M = \begin{pmatrix} A & B \\ C & D \end{pmatrix},$$

as a $(p+q) \times (p+q)$ matrix. If D is invertible, the Schur complement of the block D in M is the $p \times p$ matrix,

$$M/D := A - BD^{-1}C.$$

Similarly, if A is invertible, the Schur complement of block A is the $q \times q$ matrix,

$$M/A := D - CA^{-1}B.$$

Consequently, the inverse of M can be written in terms of the Schur complements as,

$$\begin{aligned} M^{-1} &= \begin{pmatrix} A & B \\ C & D \end{pmatrix}^{-1} \\ &= \begin{pmatrix} (M/D)^{-1} & -A^{-1}B(M/A)^{-1} \\ -D^{-1}C(M/D)^{-1} & (M/A)^{-1} \end{pmatrix}. \end{aligned}$$

C. Series expansion of the matrix inverse

Given a matrix $M = (A - B)$. We can express its inverse as,

$$\begin{aligned} M^{-1} &= (A - B)^{-1} \\ &= A^{-1} + A^{-1}B(\mathbf{I} - A^{-1}B)^{-1}A^{-1} \\ &= A^{-1} + A^{-1}B(\mathbf{I} + A^{-1}B + A^{-1}BA^{-1}B + \dots)A^{-1} \\ &= A^{-1} + A^{-1}BA^{-1} + A^{-1}BA^{-1}BA^{-1} + A^{-1}BA^{-1}BA^{-1}BA^{-1} + \dots \\ &= A^{-1}(\mathbf{I} + BA^{-1} + (BA^{-1})^2 + \dots) \end{aligned} \tag{S.10}$$

Here, from the first to the second step, we have used the Woodbury matrix identity: $(A + UCV)^{-1} = A^{-1} - A^{-1}U(\mathbf{I} + VA^{-1}U)^{-1}VA^{-1}$ with $U = -B$, $C = \mathbf{I}$, and $V = \mathbf{I}$. In the second to the third line, we have used the Neumann expansion: $(\mathbf{I} - A^{-1}B)^{-1} = \mathbf{I} + A^{-1}B + A^{-1}BA^{-1}B + \dots$.

S4. MATRIX CONTINUED FRACTION EXPANSION

We are interested in the Green's function of H_1 (Eq. S.3) projected onto $\mathbf{H}_{\text{ph},0}$. We can now use the standard techniques of matrix Green's functions for connected systems as presented in Sec. S3. Writing H_1 as,

$$H_1 = \begin{pmatrix} \mathbf{H}_{\text{ph},0} & \mathbf{V}_0 \\ \mathbf{V}_0^\dagger & \tilde{\mathbf{H}}_{e,0} \end{pmatrix}, \tag{S.11}$$

we have the photon Green's function, $D_N^R(\omega)$, as

$$D_N^R(\omega) = \frac{1}{\omega - \omega_{\text{ph}} + i\kappa/2 - \Sigma_{e,0}} \tag{S.12}$$

where

$$\Sigma_{e,0} = \mathbf{V}_0(\omega - \tilde{\mathbf{H}}_{e,0} + i\gamma/2)^{-1}\mathbf{V}_0^\dagger,$$

is the cavity self-energy due to its coupling to the $\tilde{\mathbf{H}}_{e,0}$ block. Now we can write $\tilde{\mathbf{H}}_{e,0}$ as,

$$\tilde{\mathbf{H}}_{e,0} = \begin{pmatrix} \mathbf{H}_{e,0} & \mathbf{v}_0 \\ \mathbf{v}_0^\dagger & \tilde{\mathbf{H}}_{\text{ph},1} \end{pmatrix}. \tag{S.13}$$

Using this, we can obtain $\Sigma_{e,0}$, in terms of $\Sigma_{\text{ph},1}$.

$$\Sigma_{e,0} = \mathbf{V}_0(\omega - \mathbf{H}_{e,0} + i\gamma/2 - \Sigma_{\text{ph},1})^{-1}\mathbf{V}_0^\dagger. \tag{S.14}$$

Again $\Sigma_{\text{ph},1} = \mathbf{v}_0(\omega - \mathbf{H}_{\text{ph},1} + i\kappa/2 - \Sigma_{e,1})^{-1} \mathbf{v}_0^\dagger$ is obtained in terms of the self-energy of the next step, $\Sigma_{e,1}$. Proceeding this way, we get a recursive algorithm, where the self-energy at the k^{th} step in the matrix depends on the $(k+1)^{\text{th}}$ step. Thus we have,

$$\Sigma_{e,k} = \mathbf{V}_k(\omega - \mathbf{H}_{e,k} + i\gamma/2 - \Sigma_{\text{ph},k+1})^{-1} \mathbf{V}_k^\dagger, \quad (\text{S.15a})$$

$$\Sigma_{\text{ph},k+1} = \mathbf{v}_k(\omega - \mathbf{H}_{\text{ph},k+1} + i\kappa/2 - \Sigma_{e,k+1})^{-1} \mathbf{v}_k^\dagger, \quad (\text{S.15b})$$

as the recursion relations for $0 \leq k < N$. For finite N , the series truncates at $\Sigma_{\text{ph},N} = \mathbf{v}_{N-1}(\omega - \mathbf{H}_{\text{ph},N} + i\kappa/2)^{-1} \mathbf{v}_{N-1}^\dagger$.

S5. REDUCIBLE AND IRREDUCIBLE FEYNMAN DIAGRAMS

Defining

$$\mathcal{I}(\omega', \Gamma) = \frac{1}{\omega - \omega' + i\Gamma/2}, \quad (\text{S.16})$$

we have the explicit expressions for the ‘Rayleigh’ and ‘Raman’ nonlinear susceptibilities of the molecules, $\chi_N^{2l+1}(\sum_{l=1}^{2l+1} \omega_l, \dots, \omega_1)$ [18] as,

$$\begin{aligned} \left(\frac{\omega_{\text{ph}}}{2}\right) \chi_N^{(1)}(\omega) &= -\mathbf{V}_0 \mathbf{G}_{e,0} \mathbf{V}_0^\dagger \\ &= -\sum_{m_e} \mu_{0_g m_e} \lambda \sqrt{N} \mathcal{I}(\omega_e + m_e, \gamma) \lambda \sqrt{N} \mu_{m_e 0_g}, \end{aligned} \quad (\text{S.17a})$$

$$\begin{aligned} \left(\frac{\omega_{\text{ph}}}{2}\right)^2 \chi_N^{(3)}(\omega, \omega - \omega_{\text{ph}}, \omega) &= -\mathbf{V}_0 \mathbf{G}_{e,0} \mathbf{v}_0 \mathbf{G}_{\text{ph},1} \mathbf{v}_0^\dagger \mathbf{G}_{e,0} \mathbf{V}_0^\dagger \\ &= -\sum_{m_e, m'_e, m_g} \lambda \sqrt{N} \mu_{0_g m'_e} \mathcal{I}(\omega_e + m'_e, \gamma) \lambda \mu_{m'_e m_g} \mathcal{I}(\omega_{\text{ph}} + m_g, \kappa) \\ &\quad \times \lambda \mu_{m_g m_e} \mathcal{I}(\omega_e + m_e, \gamma) \lambda \sqrt{N} \mu_{m_e 0_g}, \end{aligned} \quad (\text{S.17b})$$

$$\begin{aligned} \left(\frac{\omega_{\text{ph}}}{2}\right)^3 \chi_N^{(5)}(\{\omega, \omega - \omega_{\text{ph}}\}^2, \omega) &= -\mathbf{V}_0 \mathbf{G}_{e,0} \mathbf{v}_0 \mathbf{G}_{\text{ph},1} \mathbf{v}_0^\dagger \mathbf{G}_{e,0} \mathbf{v}_0 \mathbf{G}_{\text{ph},1} \mathbf{v}_0^\dagger \mathbf{G}_{e,0} \mathbf{V}_0^\dagger \\ &\quad - \mathbf{V}_0 \mathbf{G}_{e,0} \mathbf{v}_0 \mathbf{G}_{\text{ph},1} \mathbf{V}_1 \mathbf{G}_{e,1} \mathbf{V}_1^\dagger \mathbf{G}_{\text{ph},1} \mathbf{v}_0^\dagger \mathbf{G}_{e,0} \mathbf{V}_0^\dagger \\ &= -\sum_{m_e, m'_e, m''_e, m_g, m'_g} \lambda \sqrt{N} \mu_{0_g m''_e} \mathcal{I}(\omega_e + m''_e, \gamma) \lambda \mu_{m''_e m'_g} \mathcal{I}(\omega_{\text{ph}} + m'_g, \kappa) \lambda \mu_{m'_g m_e} \\ &\quad \times \mathcal{I}(\omega_e + m'_e, \gamma) \lambda \mu_{m'_e m_g} \mathcal{I}(\omega_{\text{ph}} + m_g, \kappa) \lambda \mu_{m_g m_e} \mathcal{I}(\omega_e + m_e, \gamma) \lambda \sqrt{N} \mu_{m_e 0_g} \\ &\quad - \sum_{m_e, m'_e, m''_e, m_g} \lambda \sqrt{N} \mu_{0_g m''_e} \mathcal{I}(\omega_e + m''_e, \gamma) \lambda \mu_{m''_e m_g} \mathcal{I}(\omega_{\text{ph}} + m_g, \kappa) \\ &\quad \times \left(\lambda \sqrt{N-1} \mu_{0_g m'_e} \mathcal{I}(\omega_e + m_g + m'_e, \gamma) \lambda \sqrt{N-1} \mu_{m'_e 0_g} \right) \\ &\quad \times \mathcal{I}(\omega_{\text{ph}} + m_g, \kappa) \lambda \mu_{m_g m_e} \mathcal{I}(\omega_e + m_e, \gamma) \lambda \sqrt{N} \mu_{m_e 0_g}. \end{aligned} \quad (\text{S.17c})$$

We return to equations for the second, fourth, and sixth order terms in the Dyson series of $D_N^R(\omega)$ and rewrite them in terms of the aforementioned nonlinear susceptibilities.

$D_N^{R,(2)}(\omega)$	Dyson series terms	Using nonlinear susceptibilities
	$\mathbf{G}_{\text{ph},0} \left(\mathbf{V}_0 \mathbf{G}_{e,0} \mathbf{V}_0^\dagger \right) \mathbf{G}_{\text{ph},0}$	$\mathbf{G}_{\text{ph},0} \left[- \left(\frac{\omega_{\text{ph}}}{2} \right) \chi_N^{(1)}(\omega) \right] \mathbf{G}_{\text{ph},0}$

$D_N^{R,(4)}(\omega)$	Dyson series terms	Using nonlinear susceptibilities
	$\mathbf{G}_{\text{ph},0} \cdot \left(\mathbf{V}_0 \mathbf{G}_{e,0} \mathbf{V}_0^\dagger \mathbf{G}_{\text{ph},0} \right)^2$	$\mathbf{G}_{\text{ph},0} \cdot \left[- \left(\frac{\omega_{\text{ph}}}{2} \right) \chi_N^{(1)}(\omega) \mathbf{G}_{\text{ph},0} \right]^2$
	$\mathbf{G}_{\text{ph},0} \left(\mathbf{V}_0 \mathbf{G}_{e,0} \mathbf{v}_0 \mathbf{G}_{\text{ph},1} \mathbf{v}_0^\dagger \mathbf{G}_{e,0} \mathbf{V}_0^\dagger \right) \mathbf{G}_{\text{ph},0}$	$\mathbf{G}_{\text{ph},0} \left[- \left(\frac{\omega_{\text{ph}}}{2} \right)^2 \chi_N^{(3)}(\omega, \omega - \omega_{\text{ph}}, \omega) \right] \mathbf{G}_{\text{ph},0}$

$D_N^{R,(6)}(\omega)$	Dyson series terms	Using nonlinear susceptibilities
	$\mathbf{G}_{\text{ph},0} \left(\mathbf{V}_0 \mathbf{G}_{e,0} \mathbf{V}_0^\dagger \mathbf{G}_{\text{ph},0} \right)^3$	$\mathbf{G}_{\text{ph},0} \left[- \left(\frac{\omega_{\text{ph}}}{2} \right) \chi_N^{(1)}(\omega) \mathbf{G}_{\text{ph},0} \right]^3$
	$\mathbf{G}_{\text{ph},0} \left(\mathbf{V}_0 \mathbf{G}_{e,0} \mathbf{V}_0^\dagger \right) \mathbf{G}_{\text{ph},0} \left(\mathbf{V}_0 \mathbf{G}_{e,0} \mathbf{v}_0 \mathbf{G}_{\text{ph},1} \mathbf{v}_0^\dagger \mathbf{G}_{e,0} \mathbf{V}_0^\dagger \right) \mathbf{G}_{\text{ph},0}$	$\mathbf{G}_{\text{ph},0} \left[- \left(\frac{\omega_{\text{ph}}}{2} \right) \chi_N^{(1)}(\omega) \mathbf{G}_{\text{ph},0} \left[- \left(\frac{\omega_{\text{ph}}}{2} \right)^2 \chi_N^{(3)}(\omega, \omega - \omega_{\text{ph}}, \omega) \right] \mathbf{G}_{\text{ph},0} \right]$
	$\mathbf{G}_{\text{ph},0} \left(\mathbf{V}_0 \mathbf{G}_{e,0} \mathbf{v}_0 \mathbf{G}_{\text{ph},1} \mathbf{v}_0^\dagger \mathbf{G}_{e,0} \mathbf{V}_0^\dagger \right) \mathbf{G}_{\text{ph},0} \left(\mathbf{V}_0 \mathbf{G}_{e,0} \mathbf{V}_0^\dagger \right) \mathbf{G}_{\text{ph},0}$	$\mathbf{G}_{\text{ph},0} \left[- \left(\frac{\omega_{\text{ph}}}{2} \right)^2 \chi_N^{(3)}(\omega, \omega - \omega_{\text{ph}}, \omega) \right] \mathbf{G}_{\text{ph},0} \left[- \left(\frac{\omega_{\text{ph}}}{2} \right) \chi_N^{(1)}(\omega) \right] \mathbf{G}_{\text{ph},0}$
	$\mathbf{G}_{\text{ph},0} \left(\mathbf{V}_0 \mathbf{G}_{e,0} \mathbf{v}_0 \mathbf{G}_{\text{ph},1} \mathbf{v}_0^\dagger \mathbf{G}_{e,0} \mathbf{v}_0 \mathbf{G}_{\text{ph},1} \mathbf{v}_0^\dagger \mathbf{G}_{e,0} \mathbf{V}_0^\dagger \right) \mathbf{G}_{\text{ph},0}$ + $\mathbf{G}_{\text{ph},0} \left(\mathbf{V}_0 \mathbf{G}_{e,0} \mathbf{v}_0 \mathbf{G}_{\text{ph},1} \mathbf{v}_1 \mathbf{G}_{e,1} \mathbf{v}_1^\dagger \mathbf{G}_{\text{ph},1} \mathbf{v}_0^\dagger \mathbf{G}_{e,0} \mathbf{V}_0^\dagger \right) \mathbf{G}_{\text{ph},0}$	$\mathbf{G}_{\text{ph},0} \left[- \left(\frac{\omega_{\text{ph}}}{2} \right)^3 \chi_N^{(5)}(\omega, \omega - \omega_{\text{ph}}, \omega, \omega - \omega_{\text{ph}}, \omega) \right] \mathbf{G}_{\text{ph},0}$

Note that amongst the two terms contributing to $\left(\frac{\omega_{\text{ph}}}{2} \right)^3 \chi_N^{(5)}(\{\omega, \omega - \omega_{\text{ph}}\}^2, \omega)$, the first term is penalized by $1/N^2$ and the second term by $1/N$. All the nonlinear susceptibilities explicitly presented in Eq. S.17 have been pictorially shown as ladder diagrams for a three-level system in Fig. 3, main text.

The above tables reveal that some of the terms at a given order can be factored into terms of lower-order molecular nonlinear susceptibilities. We call these DS-FDs/CUT-E diagrams as *reducible* diagrams. The others are called *irreducible* diagrams, and the corresponding molecular susceptibilities are the *irreducible* nonlinear susceptibilities. We saw from the rules for the CUT-E diagram rules presented in Sec. S2 that a complete diagram has to start from $\mathbf{H}_{\text{ph},0}$ and end at $\mathbf{H}_{\text{ph},0}$. This result leads to the fact that the diagrams that reach $\mathbf{H}_{\text{ph},0}$ at an intermediate step are always factorizable into diagrams of lower orders. This observation can be explicitly seen in the abovementioned examples and can be checked for higher-order terms in the Dyson series: the reducible terms contributing to $D_N^{R,(k)}(\omega)$ contain $\mathbf{G}_{\text{ph},0}$ in between, while the irreducible ones only contain $\mathbf{G}_{\text{ph},0}$ at the beginning and at the end. We will next show that the self-energy term in $D_N^R(\omega)$ is a sum over all the *irreducible* nonlinear susceptibilities, up to some constants.

A. The self-energy, $\Sigma_{e,0}$, is constituted by all the *irreducible* nonlinear susceptibilities of an N molecular ensemble

The self-energy term in $D_N^R(\omega)$, Eq. S.12 for an N ensemble, according to the matrix continued fraction expansion, Eq. S.10, is given as,

$$\Sigma_{e,0}(\omega) = \mathbf{V}_0 \frac{1}{\omega - \mathbf{H}_{e,0} - \mathbf{v}_0^\dagger \frac{1}{\omega - \mathbf{H}_{\text{ph},1} + i\kappa/2 - \mathbf{V}_1^\dagger \frac{1}{\omega - \mathbf{H}_{\text{ph},2} + i\kappa/2 - \mathbf{V}_2^\dagger \frac{1}{\omega - \mathbf{H}_{\text{ph},3} + i\kappa/2 - \mathbf{V}_3^\dagger \frac{1}{\omega - \mathbf{H}_{\text{ph},4} + i\kappa/2 - \mathbf{V}_4^\dagger \frac{1}{\omega - \mathbf{H}_{\text{ph},5} + i\kappa/2 - \mathbf{V}_5^\dagger \frac{1}{\omega - \mathbf{H}_{\text{ph},N-1} + i\gamma/2 - \mathbf{v}_N^\dagger \frac{1}{\omega - \mathbf{H}_{\text{ph},N} + i\kappa/2} \mathbf{v}_N} \mathbf{V}_1 \mathbf{v}_0} \mathbf{V}_0^\dagger} \quad (\text{S.18})$$

On the other hand, we have the result that the sum over the *irreducible* nonlinear susceptibilities computed diagrammatically using the CUT-E diagram and the rules, given as a nested summation,

$$\sum_{l=0}^{\infty} \left(\frac{\omega_{\text{ph}}}{2} \right)^l \chi_N^{(2l+1)}(\{\omega, \omega - \omega_{\text{ph}}\}^l, \omega) = - \sum_{n_{e,0}=0}^{\infty} \sum_{n_{\text{ph},1}=0}^{\infty} \cdots \sum_{n_{\text{ph},N}=0}^{\infty} \mathbf{V}_0 \mathbf{G}_{e,0} \left[\mathbf{v}_0 \mathbf{G}_{\text{ph},1} \left[\mathbf{V}_1 \mathbf{G}_{e,1} \left[\cdots \left[\mathbf{v}_N \cdot \mathbf{G}_{\text{ph},N} \mathbf{v}_N^\dagger \mathbf{G}_{e,N-1} \right]^{n_{\text{ph},N}} \cdots \right] \mathbf{V}_1^\dagger \mathbf{G}_{\text{ph},1} \right]^{n_{\text{ph},1}} \mathbf{v}_0^\dagger \mathbf{G}_{e,0} \right]^{n_{e,0}} \mathbf{V}_0^\dagger. \quad (\text{S.19})$$

This result can be explicitly checked by the reader by isolating the pathways that start and end at $\mathbf{H}_{\text{ph},0}$, and do not involve $\mathbf{H}_{\text{ph},0}$ in between, in other words, they must have \mathbf{V}_0 and \mathbf{V}_0^\dagger only in the left and right, respectively (see Sec. S5). We notice that series constitutes a nested matrix geometric progression. Repeatedly using Eq. S.10, we arrive at the fact that Eq. S.19 is equal to Eq. S.18.

S6. $\mathcal{O}(N^{-k})$ EXPANSION

Expanding $D_N^R(\omega) = \sum_{k=1}^{\infty} d_{n,k}(\omega)$ (see main text, $1/N$ expansion) where $d_{n,k}(\omega) \propto 1/N^k$, we can explicitly find $d_{n,k}(\omega)$ for $k = 0, 1$ as follows.

a. $d_{N,0}(\omega)$: This term is proportional to N^0 , so it must not have the participation of any $\mathbf{v}_k \propto 1/\sqrt{N}$,

$$d_{N,0}(\omega) = \frac{1}{\omega - \omega_{\text{ph}} + i\kappa/2 - \mathbf{V}_0 \mathbf{G}_{e,0} \mathbf{V}_0^\dagger} \quad (\text{S.20})$$

$$= \sum_{n_{e,0}=0}^{\infty} \mathbf{G}_{\text{ph},0} \left(\mathbf{V}_0 \mathbf{G}_{e,0} \mathbf{V}_0^\dagger \mathbf{G}_{\text{ph},0} \right)^{n_{e,0}}, \quad (\text{S.21})$$

used Eq. S.10 to go from the first to the second row, the latter indicates that $d_{N,0}$ is the sum over all possible paths in the CUT-E diagram restricted to the zeroth-order box.

b. $d_{N,1}(\omega)$: Truncating Eq. S.18 at $\mathbf{H}_{e,1}$ gives an $\mathcal{O}(1/N)$ expression for $D_N^R(\omega)$, $\mathcal{D}_{\mathcal{O}(1/N)}(\omega)$

$$\mathcal{D}_{\mathcal{O}(1/N)}(\omega) = \frac{1}{\omega - \omega_{\text{ph}} + i\kappa/2 - \mathbf{V}_0 \frac{1}{\omega - \mathbf{H}_{e,0} - \mathbf{v}_0^\dagger \frac{1}{\omega - \mathbf{H}_{\text{ph},1} + i\kappa/2 - \mathbf{V}_1^\dagger \frac{1}{\omega - \mathbf{H}_{e,1} + i\gamma/2} \mathbf{V}_1} \mathbf{v}_0} \mathbf{V}_0^\dagger}. \quad (\text{S.22})$$

Converting the continued fractions to summations and isolating the part of the summation **containing** $d_{N,1}(\omega)$,

$$\tilde{\mathcal{D}}_{\mathcal{O}(1/N)}(\omega) = \sum_{n_{e,0}=0}^{\infty} \mathbf{G}_{\text{ph},0} \left(\mathbf{V}_0 \mathbf{G}_{e,0} \left[\underbrace{\mathbf{I} + \mathbf{v}_0 \mathbf{G}_{\text{ph},1} \left(\mathbf{I} - \mathbf{V}_1 \mathbf{G}_{e,1} \mathbf{V}_1^\dagger \mathbf{G}_{\text{ph},1} \right)^{-1} \mathbf{v}_0^\dagger \mathbf{G}_{e,0}}_{\mathbf{X}} \right] \mathbf{V}_0^\dagger \mathbf{G}_{\text{ph},0} \right)^{n_{e,0}}.$$

The collective term in the Green's function is given by the sum of the \mathbf{X}^0 terms, which we can see yields Eq. S.20 for $d_{N,0}(\omega)$. To obtain the $+1/N$ order correction, $d_{N,1}(\omega)$, we focus on the terms linear in \mathbf{X} . Note that the terms $\mathbf{V}_0 \mathbf{G}_{e,0} \mathbf{V}_0^\dagger \mathbf{G}_{\text{ph},0}$, $\mathbf{V}_0 \mathbf{G}_{e,0} \mathbf{X} \mathbf{V}_0^\dagger \mathbf{G}_{\text{ph},0}$, and $\mathbf{G}_{\text{ph},0}$ are complex numbers and hence commute. Looking at a particular $n_{e,0}$, the term linear in $\mathbf{V}_0 \mathbf{G}_{e,0} \mathbf{X} \mathbf{V}_0^\dagger \mathbf{G}_{\text{ph},0}$ is $n_{e,0} (\mathbf{V}_0 \mathbf{G}_{e,0} \mathbf{V}_0^\dagger \mathbf{G}_{\text{ph},0})^{n_{e,0}-1} (\mathbf{V}_0 \mathbf{G}_{e,0} \mathbf{X} \mathbf{V}_0^\dagger \mathbf{G}_{\text{ph},0})$. Thus,

$$\begin{aligned} d_{N,1}(\omega) &= \mathbf{G}_{\text{ph},0} \sum_{n_{e,0}=0}^{\infty} n_{e,0} (\mathbf{V}_0 \mathbf{G}_{e,0} \mathbf{V}_0^\dagger \mathbf{G}_{\text{ph},0})^{n_{e,0}-1} (\mathbf{V}_0 \mathbf{G}_{e,0} \mathbf{X} \mathbf{V}_0^\dagger \mathbf{G}_{\text{ph},0}) \\ &= \mathbf{G}_{\text{ph},0} \sum_{n_{e,0}=0}^{\infty} \frac{d}{d(\mathbf{V}_0 \mathbf{G}_{e,0} \mathbf{V}_0^\dagger \mathbf{G}_{\text{ph},0})} (\mathbf{V}_0 \mathbf{G}_{e,0} \mathbf{V}_0^\dagger \mathbf{G}_{\text{ph},0})^{n_{e,0}} (\mathbf{V}_0 \mathbf{G}_{e,0} \mathbf{X} \mathbf{V}_0^\dagger \mathbf{G}_{\text{ph},0}) \\ &= d_{n,0}(\omega) \cdot \mathbf{V}_0 \mathbf{G}_{e,0} \mathbf{v}_0 (\omega - \mathbf{H}_{\text{ph},1} + i\kappa/2 - \mathbf{V}_1 \mathbf{G}_{e,1} \mathbf{V}_1^\dagger)^{-1} \mathbf{v}_0^\dagger \mathbf{G}_{e,0} \mathbf{V}_0^\dagger \cdot d_{n,0}(\omega). \end{aligned}$$

c. $d_{N,2}(\omega)$: Truncating Eq. S.18 at $\mathbf{H}_{e,2}$ gives $D_N^R(\omega)$ up to $\mathcal{O}(1/N^2)$,

$$\mathcal{D}_{\mathcal{O}(1/N^2)}(\omega) = \frac{1}{\omega - \omega_{\text{ph}} + i\kappa/2 - \mathbf{V}_0 \frac{1}{\omega - \mathbf{H}_{e,0} - \mathbf{v}_0^\dagger \frac{1}{\omega - \mathbf{H}_{\text{ph},1} + i\kappa/2 - \mathbf{V}_1^\dagger \frac{1}{\omega - \mathbf{H}_{e,1} + i\gamma/2 - \mathbf{v}_1^\dagger \frac{1}{\omega - \mathbf{H}_{\text{ph},2} + i\kappa/2 - \mathbf{V}_2^\dagger \frac{1}{\omega - \mathbf{H}_{e,2} + i\gamma/2} \mathbf{V}_2} \mathbf{v}_1} \mathbf{V}_1} \mathbf{v}_0} \mathbf{V}_0^\dagger}. \quad (\text{S.23})$$

Converting this expression to a summation and isolating the components **containing** $d_{N,2}(\omega)$,

$$\tilde{\mathcal{D}}_{\mathcal{O}(1/N^2)}(\omega) = \sum_{n_{e,0}=0}^{\infty} \mathbf{G}_{\text{ph},0} \left(\mathbf{V}_0 \mathbf{G}_{e,0} \left[\mathbf{I} + \mathbf{v}_0 \mathbf{G}_{\text{ph},1} \sum_{n_{e,1}} \left(\mathbf{V}_1 \mathbf{G}_{e,1} (\mathbf{I} + \mathbf{Y}) \mathbf{V}_1^\dagger \mathbf{G}_{\text{ph},1} \right)^{n_{e,1}} \mathbf{v}_0^\dagger \mathbf{G}_{e,0} + \mathbf{X}^2 \right] \mathbf{V}_0^\dagger \mathbf{G}_{\text{ph},0} \right)^{n_{e,0}}, \quad (\text{S.24})$$

where $\mathbf{Y} = \mathbf{v}_1 \mathbf{G}_{\text{ph},2} \left(\mathbf{I} - \mathbf{V}_2 \mathbf{G}_{e,2} \mathbf{V}_2^\dagger \mathbf{G}_{\text{ph},2} \right)^{-1} \mathbf{v}_1^\dagger \mathbf{G}_{e,1}$. The approach to obtain $d_{N,2}(\omega)$ is to isolate the contributions

upto linear order in \mathbf{Y} from

$$\sum_{n_{e,1}} \left(\mathbf{V}_1 \mathbf{G}_{e,1} (\mathbf{I} + \mathbf{Y}) \mathbf{V}_1^\dagger \mathbf{G}_{\text{ph},1} \right)^{n_{e,1}}$$

and expand the $n_{e,0}$ exponent as a multinomial to isolate terms $\propto 1/N^2$. However, since $\mathbf{V}_1 \mathbf{G}_{e,1} \mathbf{V}_1^\dagger \mathbf{G}_{\text{ph},1}$ and $\mathbf{V}_1 \mathbf{G}_{e,1} \mathbf{Y} \mathbf{V}_1^\dagger \mathbf{G}_{\text{ph},1}$ are matrices in general; they do not commute, and hence, we need to use the following result: Consider two matrices A and B . We have,

$$(A + B)^n = A^n + B^n + \left(A^{n-1}B + A^{n-2}BA + \dots + A^{n-k-1}BA^k + \dots + BA^{n-1} \right) + \dots$$

Thus the terms linear in B can be written as, $\sum_k A^{n-k-1}BA^k$. Applying this to Eq. S.24, we obtain

$$\tilde{D}_{\mathcal{O}(1/N^2)}(\omega) \stackrel{\mathcal{O}(\mathbf{Y})}{=} \sum_{n_{e,0}=0}^{\infty} \mathbf{G}_{\text{ph},0} \left(\mathbf{V}_0 \mathbf{G}_{e,0} \left[\mathbf{I} + \mathbf{X} + \mathbf{X}^2 + \mathbf{K} \right] \mathbf{V}_0^\dagger \mathbf{G}_{\text{ph},0} \right)^{n_{e,0}}, \quad (\text{S.25})$$

where,

$$\mathbf{K} = \sum_{n_{e,1}} \sum_{k=0}^{n_{e,1}-1} \mathbf{v}_0 \mathbf{G}_{\text{ph},1} [\mathbf{V}_1 \mathbf{G}_{e,1} \mathbf{V}_1^\dagger \mathbf{G}_{\text{ph},1}]^{n_{e,1}-k-1} \cdot \left(\mathbf{V}_1 \mathbf{G}_{e,1} \mathbf{Y} \mathbf{V}_1^\dagger \mathbf{G}_{\text{ph},1} \right) [\mathbf{V}_1 \mathbf{G}_{e,1} \mathbf{V}_1^\dagger \mathbf{G}_{\text{ph},1}]^k \mathbf{v}_0^\dagger \mathbf{G}_{e,0}$$

To obtain $d_{N,2}(\omega) \propto N^{-k}$, we need to isolate the terms quadratic in \mathbf{X} , $d_{N,2}^{(1)}$ and the terms linear in \mathbf{Y} , $d_{N,2}^{(2)}$. We have,

$$\begin{aligned} d_{N,2}^{(1)}(\omega) &= \mathbf{G}_{\text{ph},0} \sum_{n_{e,0}=0}^{\infty} \binom{n_{e,0}}{2} (\mathbf{V}_0 \mathbf{G}_{e,0} \mathbf{V}_0^\dagger \mathbf{G}_{\text{ph},0})^{n_{e,0}-2} (\mathbf{V}_0 \mathbf{G}_{e,0} \mathbf{X} \mathbf{V}_0^\dagger \mathbf{G}_{\text{ph},0})^2 + \\ &\quad \mathbf{G}_{\text{ph},0} \sum_{n_{e,0}=0}^{\infty} n_{e,0} (\mathbf{V}_0 \mathbf{G}_{e,0} \mathbf{V}_0^\dagger \mathbf{G}_{\text{ph},0})^{n_{e,0}-1} (\mathbf{V}_0 \mathbf{G}_{e,0} \mathbf{X}^2 \mathbf{V}_0^\dagger \mathbf{G}_{\text{ph},0}) \\ &= \mathbf{G}_{\text{ph},0} \left[\frac{d^2}{d(\mathbf{V}_0 \mathbf{G}_{e,0} \mathbf{V}_0^\dagger \mathbf{G}_{\text{ph},0})^2} \sum_{n_{e,0}=0}^{\infty} (\mathbf{V}_0 \mathbf{G}_{e,0} \mathbf{V}_0^\dagger \mathbf{G}_{\text{ph},0})^{n_{e,0}} \right] (\mathbf{V}_0 \mathbf{G}_{e,0} \mathbf{X} \mathbf{V}_0^\dagger \mathbf{G}_{\text{ph},0})^2 + \\ &\quad \mathbf{G}_{\text{ph},0} \left[\frac{d}{d(\mathbf{V}_0 \mathbf{G}_{e,0} \mathbf{V}_0^\dagger \mathbf{G}_{\text{ph},0})} \sum_{n_{e,0}=0}^{\infty} (\mathbf{V}_0 \mathbf{G}_{e,0} \mathbf{V}_0^\dagger \mathbf{G}_{\text{ph},0})^{n_{e,0}} \right] (\mathbf{V}_0 \mathbf{G}_{e,0} \mathbf{X}^2 \mathbf{V}_0^\dagger \mathbf{G}_{\text{ph},0}) \\ &= 2\mathbf{G}_{\text{ph},0} (1 - \mathbf{V}_0 \mathbf{G}_{e,0} \mathbf{V}_0^\dagger \mathbf{G}_{\text{ph},0})^{-3} (\mathbf{V}_0 \mathbf{G}_{e,0} \mathbf{X} \mathbf{V}_0^\dagger \mathbf{G}_{\text{ph},0})^2 + \\ &\quad \mathbf{G}_{\text{ph},0} (1 - \mathbf{V}_0 \mathbf{G}_{e,0} \mathbf{V}_0^\dagger \mathbf{G}_{\text{ph},0})^{-2} (\mathbf{V}_0 \mathbf{G}_{e,0} \mathbf{X}^2 \mathbf{V}_0^\dagger \mathbf{G}_{\text{ph},0}). \end{aligned}$$

As for $d_{N,2}^{(2)}(\omega)$, the form of the \mathbf{K} does not allow us to obtain a closed-form solution for $d_{n,2}(\omega)$. Similar challenges will be faced for $d_{n,k}(\omega)$ for $k > 2$.

-
- [S1] J. B. Pérez-Sánchez, A. Koner, S. Raghavan-Chitra, and J. Yuen-Zhou, “Cut-e as a $1/n$ expansion for multiscale molecular polariton dynamics,” (2024), [arXiv:2410.14175 \[quant-ph\]](#).
[S2] J. B. Pérez-Sánchez and J. Yuen-Zhou, “Radiative pumping vs vibrational relaxation of molecular polaritons: a bosonic mapping approach,” (2024), [arXiv:2407.20594 \[quant-ph\]](#).
[S3] A. Pizzi, A. Gorlach, N. Rivera, A. Nunnenkamp, and I. Kaminer, “Light emission from strongly driven many-body systems,” *Nature Physics* **19**, 551–561 (2023).
[S4] L. Biedenharn and H. Van Dam, *Quantum Theory of Angular Momentum: A Collection of Reprints and Original Papers*, Perspectives in Physics: a Series of Reprint Collections (Academic Press, 1965).

- [S5] M. R. Philpott, “Theory of the Coupling of Electronic and Vibrational Excitations in Molecular Crystals and Helical Polymers,” *J. Chem. Phys.* **55**, 2039–2054 (1971).
- [S6] F. C. Spano and H. Yamagata, “Vibronic coupling in j-aggregates and beyond: a direct means of determining the exciton coherence length from the photoluminescence spectrum,” *The Journal of Physical Chemistry B* **115**, 5133–5143 (2011).
- [S7] W. H. Butler, “Self-consistent cluster theory of disordered alloys,” *Phys. Rev. B* **8**, 4499–4510 (1973).
- [S8] H. M. Pastawski, J. F. Weisz, and S. Albornoz, “Matrix continued-fraction calculation of localization length,” *Phys. Rev. B* **28**, 6896–6903 (1983).
- [S9] H. M. Pastawski and J. A. Gascón, “Nmr line shape in metallic nanoparticles: A matrix continued fractions evaluation,” *Phys. Rev. B* **56**, 4887–4892 (1997).
- [S10] D. F. Martinez, “Floquet–green function formalism for harmonically driven hamiltonians,” *Journal of Physics A: Mathematical and General* **36**, 9827 (2003).
- [S11] P. Hänggi, *Driven quantum systems* (2018).
- [S12] P. Hänggi, F. Rösel, and D. Trautmann, “Continued fraction expansions in scattering theory and statistical non-equilibrium mechanics,” *Zeitschrift für Naturforschung A* **33**, 402–417 (1978).
- [S13] C. Dunezky and R. E. Wyatt, “Lanczos recursion, continued fractions, Padé approximants, and variational principles in quantum scattering theory,” *The Journal of Chemical Physics* **89**, 1448–1463 (1988).
- [S14] W. Yang and W. H. Miller, “Block Lanczos approach combined with matrix continued fraction for the S-matrix Kohn variational principle in quantum scattering,” *The Journal of Chemical Physics* **91**, 3504–3508 (1989).
- [S15] J. B. Pérez-Sánchez, A. Koner, N. P. Stern, and J. Yuen-Zhou, “Simulating molecular polaritons in the collective regime using few-molecule models,” *Proceedings of the National Academy of Sciences* **120**, e2219223120 (2023).
- [S16] J. Yuen-Zhou and A. Koner, “Linear response of molecular polaritons,” *The Journal of Chemical Physics* **160**, 154107 (2024).
- [S17] J. A. Ćwik, P. Kirton, S. De Liberato, and J. Keeling, “Excitonic spectral features in strongly coupled organic polaritons,” *Physical Review A* **93**, 033840 (2016).
- [S18] S. Mukamel, *Principles of nonlinear optical spectroscopy* (Oxford University Press, 1995).
- [S19] J. Velev and W. Butler, “On the equivalence of different techniques for evaluating the green function for a semi-infinite system using a localized basis,” *Journal of Physics: Condensed Matter* **16**, R637 (2004).